Polymer 262 (2022) 125477

Contents lists available at ScienceDirect

Polymer

journal homepage: www.elsevier.com/locate/polymer

Photo-crosslinkable and ultrastable poly(1,4-butadiene) based organogel with record-high reversible elongation upon cooling and contraction upon heating

Xiaming Feng [a,b], Guoqiang Li [a,*]

[a] Department of Mechanical & Industrial Engineering, Louisiana State University, Baton Rouge, LA, 70803, United States
[b] College of Materials Science and Engineering, Chongqing University, 174 Shazhengjie, Shapingba, Chongqing, 400044, China

ARTICLE INFO

Keywords:
poly(1,4-butadiene)
Organogels
Shape memory property
Strain sensor

ABSTRACT

Two-way shape memory polymers with reversible elongation upon cooling (EUC) and contraction upon heating (CUH) have emerged as promising smart materials for use in soft actuators. However, it remains challenging to develop organogels with as high as possible actuation strain. Here, novel photo-crosslinkable poly(1,4-butadiene) (PBD) based organogels with exceptional stability and high reversible EUC and CUH have been developed for the first time. The conventional photo-initiator 2-hydroxy-2-methylpropiophenone and plasticizer bis(2-ethylhexyl) phthalate were utilized to achieve photo-crosslinking ability and to serve as the organic free phase, respectively. Owing to the stability of the plasticizer, the PBD based organogels are pretty stable in high vacuum environment and below 100 °C. Importantly, the PBD organogel with 60 wt % plasticizer exhibited the best overall performance, especially with the record-high EUC (156%) and CUH (151%), and the pretty high actuation reversibility (97%). Moreover, the high stretchability makes the PBD based organogels possess great potential in strain sensing application. The widely accessible raw materials and simple preparation method make PBD based organogels with good possibility in practical applications.

1. Introduction

Shape memory polymers are smart materials that can be shaped into temporary forms and recover the permanent shapes by external trigger on demand [1–3]. Thermally triggered shape memory effect is particularly useful and widely studied because it is easy to achieve and no extra structures are needed [4,5]. As for two-way shape memory effect, its primary actuation feature is thermally opposite to common physics. Namely, two-way shape memory polymer expands upon cooling and contracts upon heating [6]. The two-way shape memory effect was first observed in liquid crystalline elastomers in 2001 [7]. Then, Mather et al. reported the two-way shape memory effect in a crosslinked semi-crystalline polymer network - poly(cyclooctene) [8]. After that, various two-way shape memory polymer systems with varying actuation strains and working temperature ranges have been developed, such as poly (caprolactone) [9–13], ionomers [14,15], poly(octylene adipate) [16,17], poly(ethylene-co-vinyl acetate) [18,19], polyurethane [20,21], and poly(1,4-butadiene) [6,22,23].

Polymer gels are soft and stretchable, which is composed of polymer networks swollen with small molecules [24–26], such as water for hydrogels, ionic liquid for ionogels, and organic solvent for organogels. Compared to the hydrogels and ionogels, organogels are more stable to thermal and moisture change due to the stability of organic solvents, which present more feasibilities in wide applications [27–29]. Generally, organogels can be prepared by swelling crosslinked polymers in organic solvents. However, the obtained organogels are sometimes inhomogeneous because of the concentration gradient with depth. In-situ polymerization of monomer/oligomer in organic solvents is an effective method to fabricate homogeneous organogels. Among all the polymerization methods, the photo-induced polymerization/crosslinking is feasible in practical usage, which is energy-saving and can be achieved in minutes instead of hours or days [27,30]. Moreover, the photo induced crosslinking can be easily modified for 3D printing.

Stimuli-responsive gels have attracted more and more attentions due to the unique properties and smart features [31,32]. Tremendous efforts have been devoted to develop various functional gels, such as hydrogels for drug release and ionogels for strain sensing [28,33]. Indeed, some

* Corresponding author.
E-mail address: lguoqi1@lsu.edu (G. Li).

https://doi.org/10.1016/j.polymer.2022.125477
Received 22 July 2022; Received in revised form 27 October 2022; Accepted 28 October 2022
Available online 1 November 2022

shape memory polymer gels have been reported recently [34]. For example, Zhao et al. developed a highly stretchable, shape memory organohydrogels by utilizing phase-transition micro inclusions [35]. Cai and coworkers demonstrated a high strength, recyclable, anti-swelling and shape-memory hydrogels based on crystal microphase crosslinking for flexible sensor applications [36]. However, few reports focus on the two-way shape memory properties of polymer gels. In our previous report [6], a thermally crosslinked poly(1,4-butadiene) material have been synthesized with giant reversible elongation upon cooling and contraction upon heating at temperatures below zero Celsius. Both entropy and enthalpy mechanism were responsible for the reversible actuation [37]. However, the actuation strain is still not high enough. Most importantly, the actuation reversibility of this polymer is only 75%, which is quite low for long-term usage in practical applications. Therefore, it is urgent to develop a two-way shape memory system with as high as possible actuation strain and satisfied actuation reversibility.

In this work, we utilized a common plasticizer as a free organic phase to develop PBD based organogels. Owing to the incorporation of a photo-initiator, the gels can be crosslinked by UV light in several minutes. The organogels are ultrastable to high vacuum environment and high temperature. More impressively, the PBD based organogels exhibited a record-high two-way shape memory actuation strain due to the balanced melting/crystallization behavior and crosslinked molecular networks. Moreover, a potential application as strain sensing has been demonstrated. Overall, we believe a new convenient method for the fabrication of smart organogels has been proposed and validated.

2. Experimental section

2.1. Materials

Cis-poly(1,4-butadiene) (PBD) (Budene® 1208) was supplied by Goodyear Chemical (Akron, OH, USA). The viscosity is 46 (Mooney ML 1 + 4 @ 100 °C) and the onset glass transition temperature is −104 °C according to our previous report [6]. Chloroform, bis(2-ethylhexyl) phthalate, and 2-hydroxy-2-methylpropiophenone (97%) were purchased from Sigma-Aldrich and used as received.

2.2. Synthesis of PBD based organogels

First, 50 g of PBD were cut into small pieces and immersed into 950 g of chloroform for at least 3 days. The conical flask was fully sealed to avoid the evaporation of chloroform. After completely swelling, the mixture was vigorously stirred for 1 h to obtain a sticky homogeneous solution. Various amounts of plasticizer bis(2-ethylhexyl) phthalate and photoinitiator 2-hydroxy-2-methylpropiophenone were added into the solution upon further stirring. Chloroform was then removed by simple evaporation and overnight vacuum drying at room temperature. Three formulas with different amounts (40, 60, and 80 wt%) of plasticizer were prepared. The content of photoinitiator is constant (3 wt% of PBD) for all formulas. After completely removing the solvent, the obtained samples were named as PBD-40P, PBD-60P, and PBD-80P corresponding to the content of the plasticizer. As for UV curing, the obtained sticky samples were smeared into a plastic spacer with thickness of 1.2 mm clamped by two transparent plastic slides. The samples were maintained until the air bubbles disappeared. The samples were then cured in a UV chamber (IntelliRay 600, Uvitron International, USA) for 60 s under 80% irradiation intensity (232 nm, ~45 mW/cm^2). The crosslinked samples were abbreviated as c-PBD-40P, c-PBD-60P, and c-PBD-80P, respectively.

For demonstrating the strain sensing application, the organogel specimen was coated with multiwalled carbon nanotubes (20–40 nm of diameter, 5–15 μm of length) to increase the electrical conductivity. Specifically, the multiwalled carbon nanotube particles were homogeneously sprayed on the surface of the PBD-60P film. The obtained sample was wrapped by PTFE films and hot-pressed at 100 °C for 2 h. Finally, the sensor specimen was treated by ultrasonic cleaning in ethanol to remove the unbounded carbon nanotubes.

2.3. Characterization

Thermal behavior of the organogels was characterized by PerkinElmer 4000 differential scanning calorimeter (DSC) (MA, USA). About 5 mg of the samples was heated and cooled between −70 and 80 °C at a rate of 10 °C min^{-1}; both the holding times at −70 and 80 °C were 2 min. The second heating-cooling cycle was conducted and profiled to remove

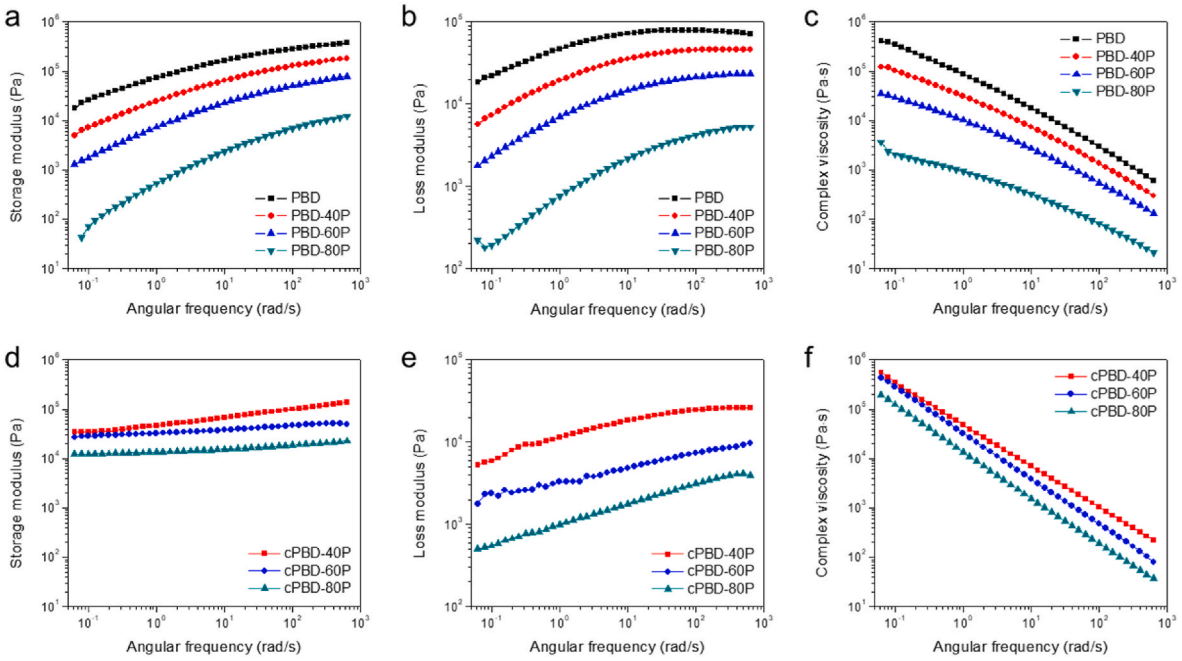

Fig. 1. (a) Storage modulus, (b) loss modulus, and (c) complex viscosity versus angular frequency for un-crosslinked pure PBD and un-crosslinked PBD with various amounts of plasticizer. (d) Storage modulus, (e) loss modulus, and (f) complex viscosity versus angular frequency for crosslinked PBD based organogels.

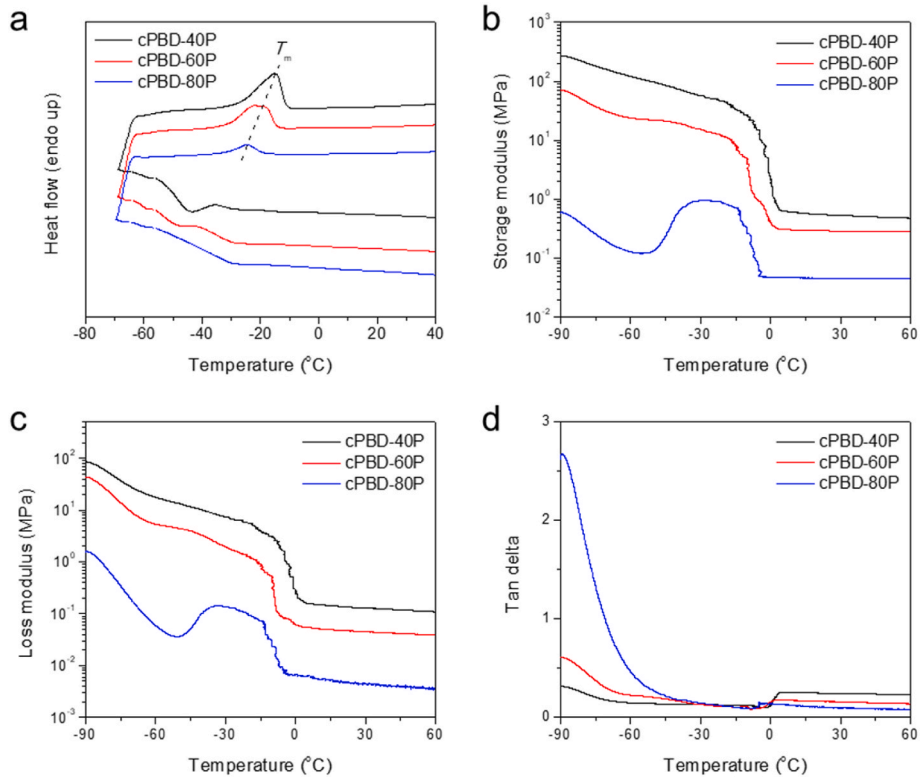

Fig. 2. Profiles of (a) heat flow, (b) storage modulus, (c) loss modulus, and (d) tan delta versus temperature for crosslinked PBD based organogels.

the effect of thermal history. The purging rate of nitrogen gas was 30 mL min^{-1}.

Storage modulus, loss modulus, and tan δ curves were collected by a Q800 dynamic mechanical analyzer (DMA) (TA Instruments, DE, United States) in multifrequency strain mode with a heating rate of 3 °C/min and a frequency of 1 Hz. The temperature range was from −90 °C to 60 °C.

Thermogravimetric analysis (TGA) was conducted by a Q5000 thermal analyzer (TA Co., USA). For non-isothermal test, the sample was heated from 25 to 800 °C at a heating rate of 10 °C/min in nitrogen atmosphere. For isothermal test, the sample was rapidly heated from 25 to 100 °C at a heating rate of 100 °C/min in nitrogen atmosphere, then isothermal at 100 °C for 120 min. The purging rate of nitrogen gas was 40 mL min^{-1}.

Tensile test of dumbbell-shaped samples (ASTM D412) was performed by an eXpert 2610 MTS (ADMET, Norwood, MA, United States). The stretching rate was 20, 100, and 500 mm/min, respectively. For loading-unloading cycle test, the stretching rate was 20 mm/min. At least three parallel samples were used for tensile test.

Two-way shape memory performance was acquired with control-force mode using the Q800 dynamic mechanical analyzer (DMA) (TA Instruments, DE, USA) according to our previous report [38]. The tensile load and temperature were preprogrammed, and the strain change can be precisely recorded. The heating and cooling rate was 5 °C min^{-1}. The isothermal time at −40 °C and 60 °C was 5 min and 3 min, respectively.

The stability of organogels was tested by drying in a vacuum oven at room temperature for various periods. The weight change was recorded by a balance.

The rheological behaviors of uncrosslinked specimens and crosslinked organogels were characterized with an HR 30 Discovery Hybrid Rheometer (TA Instruments, DE, USA) in parallel plate geometry (25 mm diameter and 1000 μm gap). Frequency sweep measurements were performed at 25 °C from 0.01 Hz to 100 Hz in dynamic mode with a strain of 1%. Stain sweep tests were performed at 25 °C from 0.01% to 100% in dynamic mode with an angular frequency of 10 rad/s.

The strain sensing properties were tested by coupling DMA (TA Instruments, DE, USA) and SourceMeter 2400 (Fotronic Co., MA). The specimen was stretched by DMA in strain rate mode at a rate of 5.0%/min to 20% and 50%, respectively. The change of electrical resistance was recorded in I–V mode by the SourceMeter 2400.

3. Results and discussions

3.1. Viscoelastic behaviors

The addition of plasticizer can obviously change the viscoelastic behaviors of polymers. The storage modulus, loss modulus, and complex viscosity for pure PBD and PBD with various amounts of plasticizer were characterized by rheometer. First, the effect of oscillation strain on viscoelastic plasticizer was studied and shown in Fig. S1 to determine the linear viscoelastic region. With increasing the content of plasticizer, the linear viscoelastic region extended to higher oscillation stain. Within the linear region, the 1% oscillation strain was selected to conduct the frequency sweep test. Fig. 1 compares the storage modulus, loss modulus, and complex viscosity of uncrosslinked and UV crosslinked PBD organogels, respectively. As shown in Fig. 1a–c, certainly, the more the plasticizer incorporated, the lower the modulus and viscosity obtained. The reduction by orders of magnitude can be observed. These results suggest that the obtained PBD gels are injectable and can be printed by the conventional UV assisted extrusion printer. Fig. 1d–e shows the results of UV crosslinked PBD organogels. Different from the uncrosslinked specimens, the moduli of crosslinked PBD organogels are not that sensitive to the angular frequency. The modulus is significantly increased after UV crosslinking, indicating the successful polymerization of the PBD organogels. Moreover, the difference between the storage modulus and complex viscosity before and after UV crosslinking is much reduced, which indicates that all the crosslinked PBD organogels have strong enough mechanical properties to be used as solid materials.

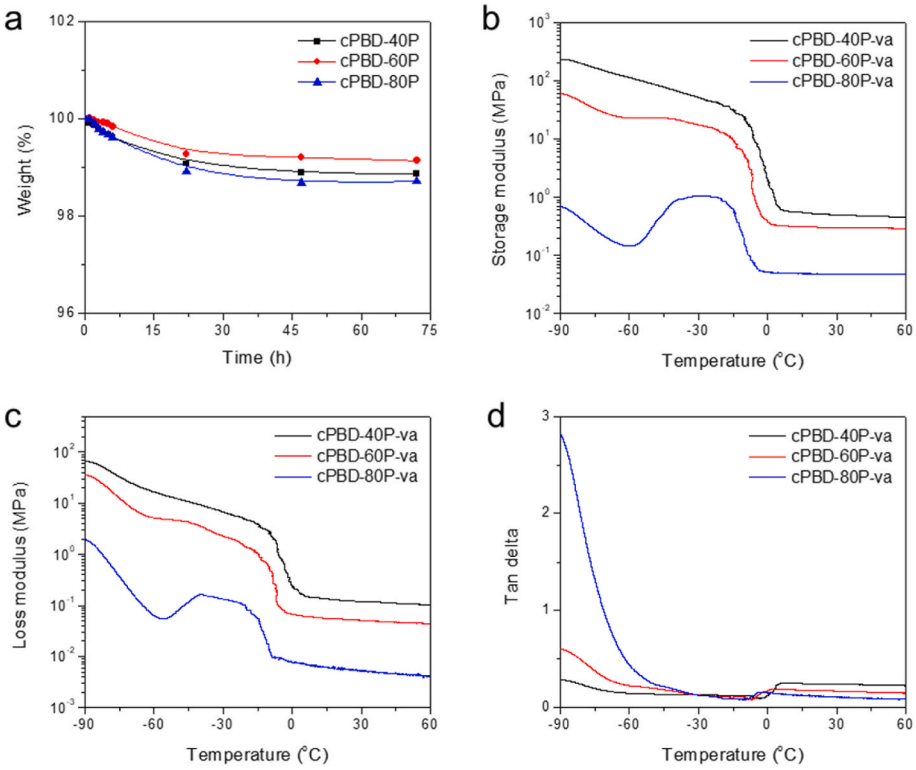

Fig. 3. (a) Weight loss of crosslinked PBD based organogels at different vacuum drying time. Profiles of (b) storage modulus, (c) loss modulus, and (d) tan delta versus temperature for crosslinked PBD based organogels after 72 h vacuum drying at room temperature.

3.2. Thermal and dynamic mechanical analysis

Thermal properties of crosslinked PBD based organogels were characterized by DSC, and the corresponding profiles were displayed in Fig. 2a. According to our previous report, the melting point (T_m) of the crosslinked PBD is −8.7 °C [6]. The addition of plasticizer gradually decreased the T_m and degree of crystallinity, as demonstrated by the left-shifted and reduced endothermic melting peaks. The T_m values for c-PBD-40P, c-PBD-60P, and c-PBD-80P are −14.8 °C, −20.4 °C, and −24.4 °C, respectively. A similar variation trend can be observed for the exothermic crystallization peaks. The large amount of small plasticizer molecules heavily restrains the rearrangement and formation of crystals for crosslinked PBD. Additionally, the modulus of PBD based organogels were dramatically decreased with adding plasticizer. Fig. 2b and c displays the storage modulus and loss modulus of the specimens. One can see that the c-PBD-80P sample exhibits the lowest storage modulus and loss modulus, which decreased by two orders of magnitude. In Fig. 2d, with increasing temperature from −90 °C to −50 °C, the tan delta value decreases, probably due to the glassy-rubbery transition of the PBD segments. Generally, the huge difference in modulus before and after the transition is a critical factor in achieving good shape memory effect.

3.3. Environmental and thermal stabilities

For the purpose of durability, the stabilities of organogels are of great importance in practical applications. The environmental stability was characterized by placing PBD based organogels in a high vacuum environment. The weight change of the organogels under 6×10^{-4} Pa environment was recorded and shown in Fig. 3a. Except for the initial weight loss caused by impurities, the weight of the samples is pretty stable after 48 h. For the highest weight loss, only 1.3% can be found for cPBD-80P specimen. Because bis(2-ethylhexyl) phthalate is nonvolatile and hydrophobic, the weight of the PBD based organogels was almost unchanged even after storing for 72 h in the vacuum environment, demonstrating that the PBD based organogels are ultrastable in open air. To better illustrate the environmental stability, the specimens after

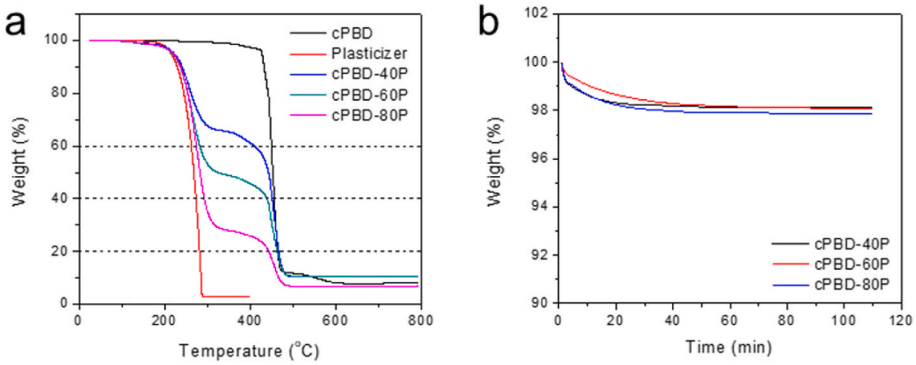

Fig. 4. (a) Non-isothermal and (b) isothermal TG curves of different samples at 100 °C.

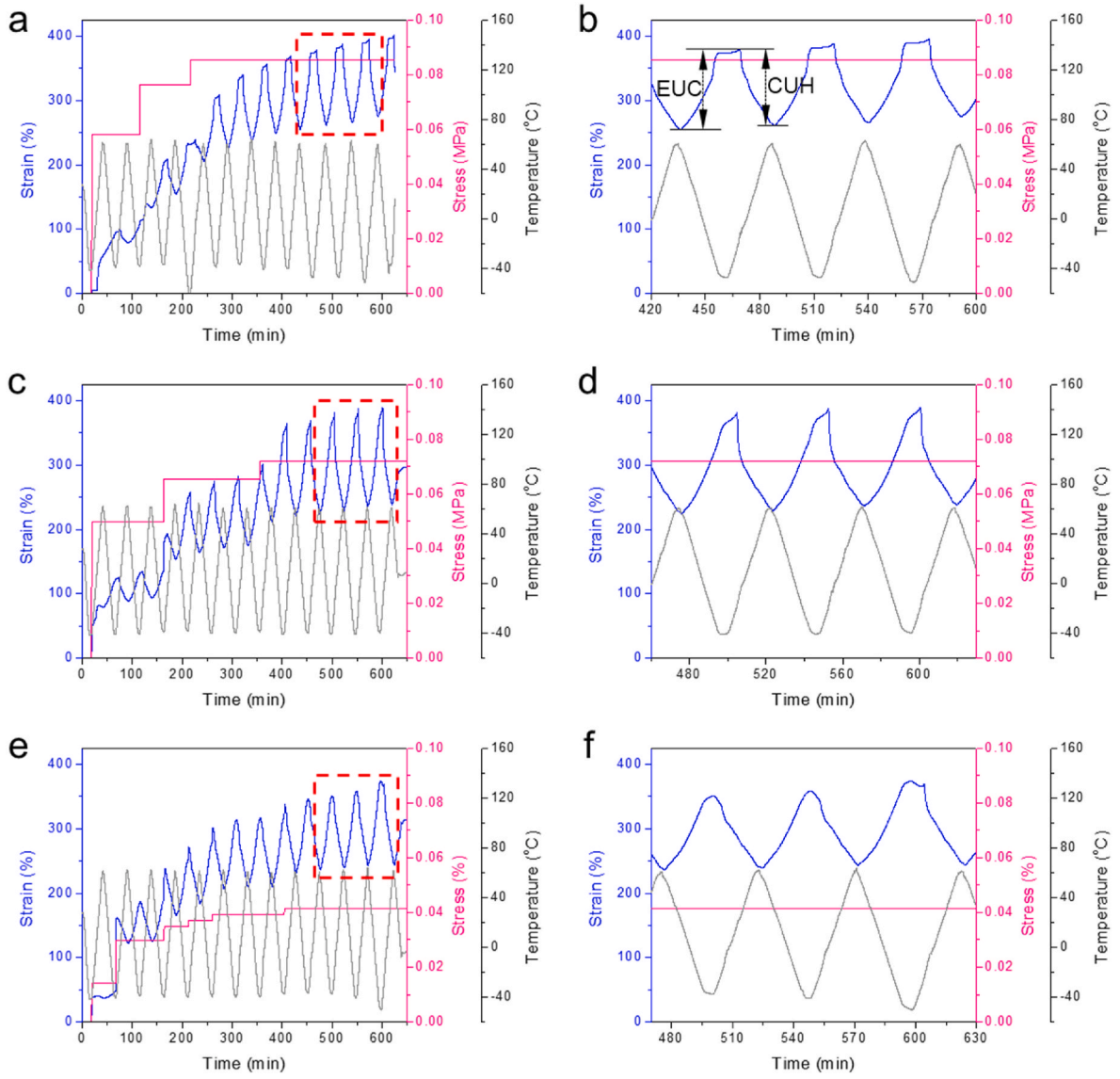

Fig. 5. Two-way shape memory properties of the (a, b) cPBD-40P, (c, d) cPBD-60P, and (e, f) cPBD-80P. The right column is the enlarged figure of each part circled by the red box on the left figures. (For interpretation of the references to colour in this figure legend, the reader is referred to the Web version of this article.)

vacuum drying for 72 h were characterized by DMA and the corresponding results are profiled in Fig. 3b–d. One can observe the highly repeatable storage modulus, loss modulus, and tan delta curves for all three samples. It suggests that the PBD based organogels can fully maintain their thermal and mechanical performance in high vacuum environment, thus leading to the ultrastability in ambient environment.

Thermal stability is another critical property for thermally triggered shape memory polymer systems. The non-isothermal test in inert atmosphere was conducted first to evaluate the thermal decomposition behaviors of PBD based organogels, as shown in Fig. 4a. Both pure cPBD and plasticizer follow a single step decomposition process, corresponding to the dissociation of backbone and main structure. For PBD based organogels, one can clearly observed two separate decomposition steps ascribed to the cPBD and plasticizer, respectively, which indicates that the addition of plasticizer rarely affects the decomposition behavior of cPBD. However, the residual weight after the first decomposition step is much higher than the theoretical value, which indicates that the cross-linked PBD networks obviously restrain the decomposition rate of plasticizer. Additionally, the isothermal test at 100 °C was performed to illustrate the thermal stability of PBD based organogels. Only ~2% weight loss can be observed after ~2 h at 100 °C, which might be attributed to the impurities. This means that the PBD based organogels have an excellent stability in consideration of the temperature window (−40 °C–60 °C) for two-way shape memory effect, which is discussed in the following section.

3.4. Two-way shape memory performance

Fig. 5 displays the two-way shape memory results that conducted between −40 °C to 60 °C subjected to a constant external force. A representative reversible elongation upon cooling and contraction upon heating effect are found. Because of the stress induced crystallization effect, within a reasonable load range, the larger the external load, the better the two-way shape memory effect, including higher elongation upon cooling (EUC) and contraction upon heating (CUH). After optimizing the external force and stabilization, at least three repeatable and stable actuation cycles can be obtained, which are highlighted by the dotted red line in Fig. 5 (a), (c) and (e), and are magnified correspondingly in Fig. 5 (b), (d) and (f). The average EUC and CUH for the cPBD-40P are 126% and 120%, respectively, and the external force is 0.085 MPa. By actuating within the same temperature range, the cPBD-60P specimen exhibited the highest actuation strain (Fig. 5b), of which

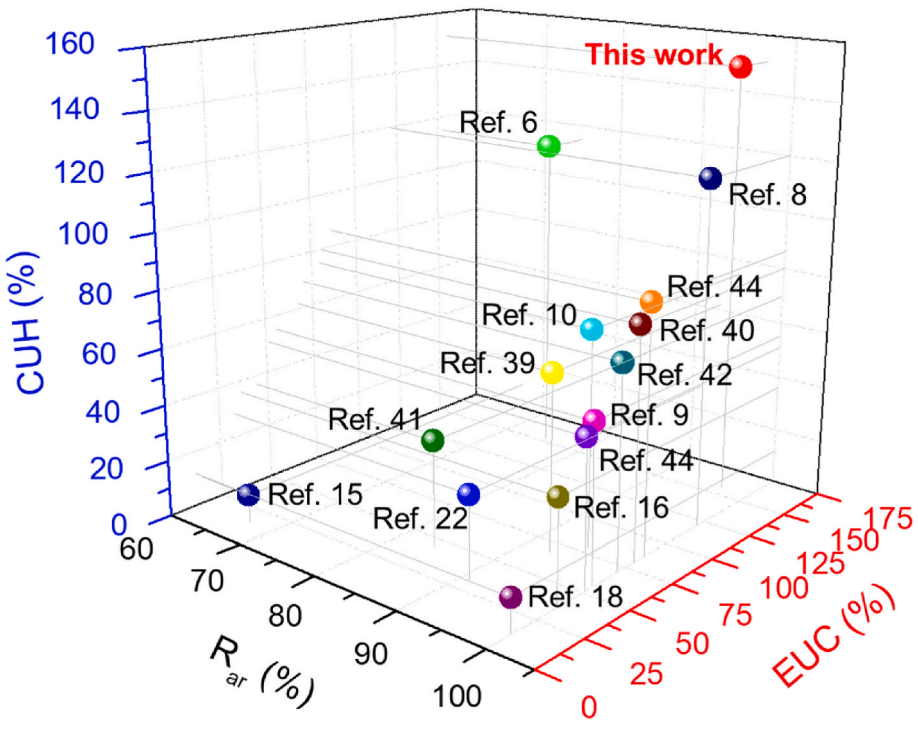

Fig. 6. Performance comparison of two-way shape memory polymers.

the EUC and CUH are 156% and 151%, respectively. When the content of plasticizer was increased to 80 wt%, lower actuation strain (121% and 119%) and lower external force (0.041 MPa) were observed. These results suggest that an optimized content of plasticizer is necessary to achieve the best two-way shape memory actuation strain. Moreover, the cPBD-60P exhibited the highest actuation stability with low strain creep. After 3 cycles (Fig. 5b, d, and 5f), the creep strain of the cPBD-60P is 9%, while those of the cPBD-40P and cPBD-80P are 17% and 22%, respectively. All these results demonstrate that the cPBD-60P specimen has the best overall two-way shape memory performance. It is believed that the giant reversible EUC and CUH of the cPBD-60P organogel is attributed to the combination effect of entropic elasticity and crystallization/melting

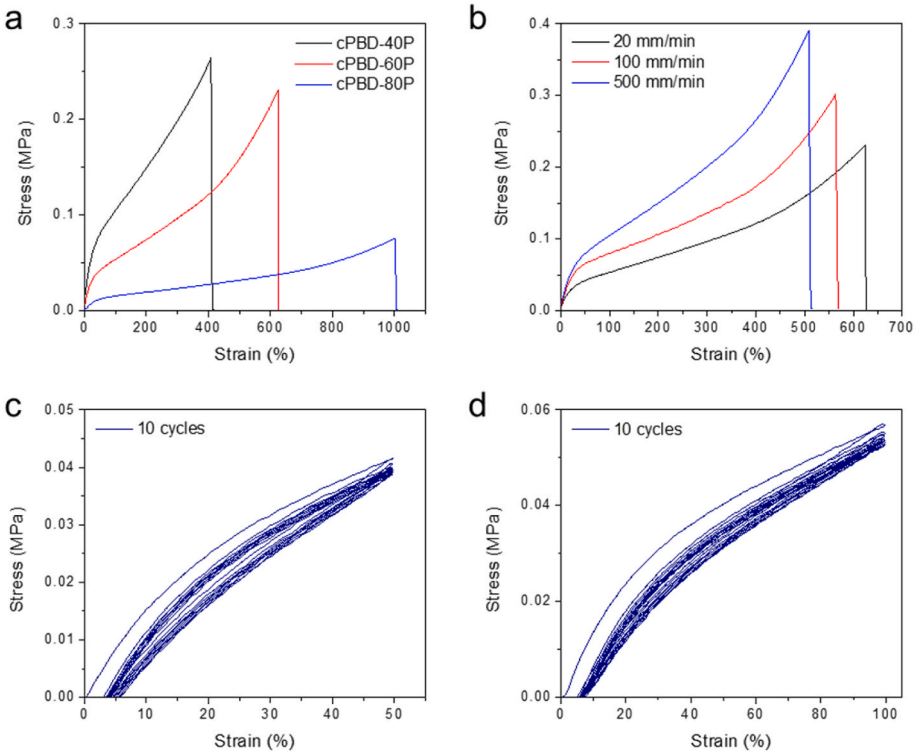

Fig. 7. Tensile stress-strain curves of (a) crosslinked PBD based organogels at stretching rate of 20 mm/min, and (b) cPBD-60P sample at different stretching rates. Loading-unloading cycle curves of cPBD-60P sample at stretching strain of (c) 50% and (d) 100%.

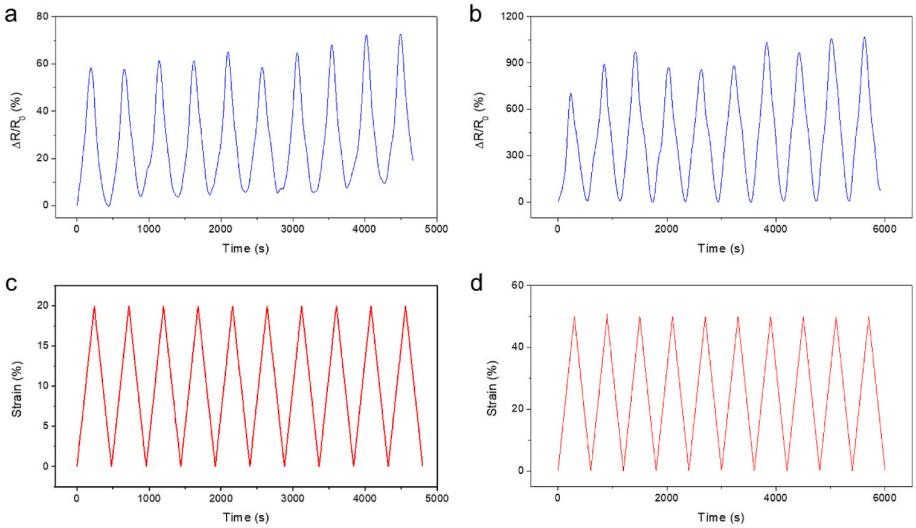

Fig. 8. (a, b) Relative resistance ratio variation of the cPBD-60P specimen during consecutive loading-unloading cycle tests under the maximum applied strain of (c) 20% and (d) 50%.

transition. It is worth mentioning that, in a previous study, Yan et al. [38] quantified the contribution of rubber elasticity and melt/crystallization on the two-way shape memory effect of PBD. They showed that in rubbery state, the two-way shape memory effect is due to rubber elasticity; at temperature below the crystallization temperature, the two-way shape memory effect is due to stress induced crystallization. Lu et al. [6] conducted in situ X-ray diffraction (XRD), Raman spectroscopy, and cryogenic scanning electron microscopy (cryo-SEM) to disclose the mechanisms controlling the two-way shape memory effect of PBD. They also showed that the increase in crystallinity as temperature drops accounts for the EUC. In this current work, although the addition of plasticizer may change the crosslinked network, it is believed that the mechanisms for the two-way shape memory effect of the organogel are similar to those of the pure PBD network. However, more direct evidences such as in-situ X-ray diffraction and Raman spectroscopy characterization should be conducted, which will be a topic of research in our future studies.

The comparison of two-way shape memory properties has been made to further validate the better performance of cPBD-60P organogel. As shown in Fig. 6, the EUC, CUH, and actuation reversibility (R_{ar}) are displayed. The R_{ar} is defined as the ratio of CUH to EUC, to evaluate the reversible actuation performance. One can see that the cPBD-60P organogel exhibited the highest CUH and EUC compared to those reported two-way shape memory systems [6,8–10,15,16,18,22,39–44]. Additionally, the R_{ar} is 97% for cPBD-60P organogel, which is comparable to the best ones. It means the cPBD-60P organogel possess record-high actuation strain and excellent reversibility at the same time. It certainly satisfies the critical requirements by soft robots demanding large actuation strain. Moreover, the temperature for triggering two-way shape memory effect of cPBD-60P organogel is much lower than most of the two-way shape memory polymers (Table S1). According to our previous report [6], the two-way shape memory polymers with reversible actuation at subzero Celsius temperatures can be used as sealant to seal joints and cracks in pavements and bridge decks. The reason is that the joints open at lower temperature and narrow at higher temperature, therefore, a sealant should behave opposite to this behavior. Other outdoor applications may also include gasket for pipelines, which are a critical component for oil and gas transport, and for singles in the roof, which are exposed to daily temperature fluctuations.

3.5. Mechanical properties

The PBD based organogels are stretchable and their mechanical properties are highly tunable by adding various amounts of plasticizer. As displayed in Fig. 7a, with increasing the content of the plasticizer, the elongation at break for the organogels increased from 409 to 999%. Certainly, the organogels exhibited monotonically decreased tensile strength (from 0.26 MPa to 0.08 MPa) and Young's modulus. Fig. 7b shows the stretching rate dependence of the tensile properties. The cPBD-60P specimen exhibited higher tensile strength and Young's modulus, but lower tensile fracture strain at a higher stretching rate. To better illustrate the mechanical performance, the cyclic loading-unloading tensile test were performed at stretching strain of 50% (Figs. 7c) and 100% (Fig. 7d), respectively. Small hysteresis loops and residual strains were observed in the loading-unloading cycles, which demonstrates the high resilience of the cPBD-60P specimen. Furthermore, except for the first cycle, the highly repeatable loading-unloading cycles indicate the stable mechanical properties and also suggest that no internal fracture of covalent bonds occurred.

3.6. Potential application as strain sensor

Due to the stretchability, one promising application of the cPBD-60P sample is to serve as a strain sensor. The electrical conductivity can be easily achieved by a simple dry coating and hot-pressing procedure. The conductive multiwalled carbon nanotubes were tightly embedded on the surface of the cPBD-60P organogel. As displayed in Fig. 8, the organogel sensor exhibited fast, reproducible, and reliable responses to small strain. After 10 loading-unloading cycles of stretching at a maximum tensile strain of 20% and 50%, respectively, the cPBD-60P organogel based sensor maintained its electrical resistance with no obvious change, suggesting the good electrical durability and dynamic electromechanical reliability. This promising performance may be used to monitor various movements, such as human motion. However, it is noted that, while 10 cycles have been conducted in this study, more cycles are needed to fully establish the stability of the organogel as strain sensors, which will be comprehensively studied in our future studies. Moreover, it is noted, in order to establish the relationship between the resistance changes and tensile strains, more strain levels should be investigated, which will be a research topic for future studies. Furthermore, although the repeatability in the sensing behavior in Fig. 8 indirectly shows that the morphology of the CNT network before and after the cyclic sensing test should be similar, direct imaging of the CNT network will better support the test results in Fig. 8.

4. Conclusions

In summary, we report a new kind of PBD based organogels with excellent stability by utilizing a commercial plasticizer as the organic phase. Specifically, the dynamic mechanical properties remain unchanged after placing the PBD based organogels in a high vacuum environment for 72 h. Owing to the melting/crystallization transition and crosslinked molecular network, the newly designed organogels exhibited a promising two-way shape memory property, which can be actuated below 0 °C with giant actuation strain. In particular, the EUC and CUH are 156% and 151% respectively, in the working temperature range of −40 to 60 °C, which are higher than those of the reported systems to the best of our knowledge. Besides the high actuation strain, the reversibility of the actuation is calculated to be 97%, demonstrating high actuation stability in practice. We believe the PBD based organogel systems can be applied in outdoor as actuators that are triggered by natural temperature change.

CRediT authorship contribution statement

Xiaming Feng: Conceptualization, Methodology, Investigation, Writing – original draft. **Guoqiang Li:** Conceptualization, Writing – review & editing, Funding acquisition, Supervision.

Declaration of competing interest

The authors declare that they have no known competing financial interests or personal relationships that could have appeared to influence the work reported in this paper.

Data availability

Data will be made available on request.

Acknowledgments

This work is supported by the US National Science Foundation under grant number OIA-1946231 and the Louisiana Board of Regents for the Louisiana Materials Design Alliance (LAMDA), and National Science Foundation under grant number HRD-1736136.

Appendix A. Supplementary data

Supplementary data to this article can be found online at https://doi.org/10.1016/j.polymer.2022.125477.

References

[1] A. Lendlein, O.E.C. Gould, Reprogrammable recovery and actuation behaviour of shape-memory polymers, Nat. Rev. Mater. 4 (2019) 116–133, https://doi.org/10.1038/s41578-018-0078-8.
[2] Y. Xia, Y. He, F. Zhang, Y. Liu, J. Leng, A review of shape memory polymers and composites: mechanisms, materials, and applications, Adv. Mater. 33 (2021), 2000713, https://doi.org/10.1002/adma.202000713.
[3] K. Wang, Y. Jia, C. Zhao, X. Zhu, Multiple and two-way reversible shape memory polymers: Design strategies and applications, Prog. Mater. Sci. 105 (2019), 100572, https://doi.org/10.1016/j.pmatsci.2019.100572.
[4] M. Zare, M.P. Prabhakaran, N. Parvin, S. Ramakrishna, Thermally-induced two-way shape memory polymers: mechanisms, structures, and applications, Chem. Eng. J. 374 (2019) 706–720, https://doi.org/10.1016/j.cej.2019.05.167.
[5] X. Feng, G. Li, High-temperature shape memory photopolymer with intrinsic flame retardancy and record-high recovery stress, Appl. Mater. Today 23 (2021), 101056, https://doi.org/10.1016/j.apmt.2021.101056.
[6] L. Lu, J. Cao, G. Li, Giant reversible elongation upon cooling and contraction upon heating for a crosslinked cis poly(1,4-butadiene) system at temperatures below zero Celsius, Sci. Rep. 8 (2018), 14233, https://doi.org/10.1038/s41598-018-32436-9.
[7] D.L. Thomsen, P. Keller, J. Naciri, R. Pink, H. Jeon, D. Shenoy, B.R. Ratna, Liquid crystal elastomers with mechanical properties of a muscle, Macromolecules 34 (2001) 5868–5875, https://doi.org/10.1021/ma001639q.
[8] T. Chung, A. Romo-Uribe, P.T. Mather, Two-way reversible shape memory in a semicrystalline network, Macromolecules 41 (2008) 184–192, https://doi.org/10.1021/ma071517z.
[9] M.R. Pfau, K.G. McKinzey, A. Roth, M.A. Grunlan, PCL-based shape memory polymer semi-IPNs: the role of miscibility in tuning the degradation rate, Biomacromolecules 21 (2020) 2493–2501, https://doi.org/10.1021/acs.biomac.0c00454.
[10] M. Huang, X. Dong, L. Wang, J. Zhao, G. Liu, D. Wang, Two-way shape memory property and its structural origin of cross-linked poly(ε-caprolactone), RSC Adv. 4 (2014) 55483–55494, https://doi.org/10.1039/C4RA09385B.
[11] N. Inverardi, S. Pandini, G. Gemmo, M. Toselli, M. Messori, G. Scalet, F. Auricchio, Reversible stress-driven and stress-free two-way shape memory effect in a sol-gel crosslinked polycaprolactone, Macromol. Symp. 405 (2022), 2100254, https://doi.org/10.1002/masy.202100254.
[12] A.P. Murcia, J.M.U. Gomez, J.-U. Sommer, L. Ionov, Two-way shape memory polymers: evolution of stress vs evolution of elongation, Macromolecules 54 (2021) 5838–5847, https://doi.org/10.1021/acs.macromol.1c00568.
[13] N. Inverardi, M. Toselli, G. Scalet, M. Messori, F. Auricchio, S. Pandini, Stress-free two-way shape memory effect of poly(ethylene glycol)/Poly(ε- caprolactone) semicrystalline networks, Macromolecules 55 (2022) 8533–8547, https://doi.org/10.1021/acs.macromol.2c01064.
[14] L. Lu, G. Li, One-way multishape-memory effect and tunable two-way shape memory effect of ionomer poly(ethylene- *co* -methacrylic acid), ACS Appl. Mater. Interfaces 8 (2016) 14812–14823, https://doi.org/10.1021/acsami.6b04105.
[15] T. Xie, J. Li, Q. Zhao, Hidden thermoreversible actuation behavior of nafion and its morphological origin, Macromolecules 47 (2014) 1085–1089, https://doi.org/10.1021/ma402203q.
[16] C.A. Tippets, Q. Li, Y. Fu, E.U. Donev, J. Zhou, S.A. Turner, A.-M.S. Jackson, V. S. Ashby, S.S. Sheiko, R. Lopez, Dynamic optical gratings accessed by reversible shape memory, ACS Appl. Mater. Interfaces 7 (2015) 14288–14293, https://doi.org/10.1021/acsami.5b02688.
[17] J. Zhou, S.A. Turner, S.M. Brosnan, Q. Li, J.-M.Y. Carrillo, D. Nykypanchuk, O. Gang, V.S. Ashby, A.V. Dobrynin, S.S. Sheiko, Shapeshifting: reversible shape memory in semicrystalline elastomers, Macromolecules 47 (2014) 1768–1776, https://doi.org/10.1021/ma4023185.
[18] M. Behl, K. Kratz, U. Noechel, T. Sauter, A. Lendlein, Temperature-memory polymer actuators, Proc. Natl. Acad. Sci. USA 110 (2013) 12555–12559, https://doi.org/10.1073/pnas.1301895110.
[19] J. Fan, G. Li, High performance and tunable artificial muscle based on two-way shape memory polymer, RSC Adv. 7 (2017) 1127–1136, https://doi.org/10.1039/C6RA25024F.
[20] M. Behl, K. Kratz, J. Zotzmann, U. Nöchel, A. Lendlein, Reversible bidirectional shape-memory polymers, Adv. Mater. 25 (2013) 4466–4469, https://doi.org/10.1002/adma.201300880.
[21] J.M. Laza, A. Veloso, J.L. Vilas, Tailoring new bisphenol a ethoxylated shape memory polyurethanes, Macromol. J. Appl. Polym. Sci. 138 (2021), e49660, https://doi.org/10.1002/app.49660.
[22] Q. Yang, W. Zheng, W. Zhao, C. Peng, J. Ren, Q. Yu, Y. Hu, X. Zhang, One-way and two-way shape memory effects of a high-strain *cis* -1,4-polybutadiene–polyethylene copolymer based dynamic network *via* self-complementary quadruple hydrogen bonding, Polym. Chem. 10 (2019) 718–726, https://doi.org/10.1039/C8PY01614C.
[23] S. Sarrafan, X. Feng, G. Li, A soft syntactic foam actuator with high recovery stress, actuation strain, and energy output, Mater. Today Commun. 31 (2022), 103303, https://doi.org/10.1016/j.mtcomm.2022.103303.
[24] P.R.A. Chivers, D.K. Smith, Shaping and structuring supramolecular gels, Nat. Rev. Mater. 4 (2019) 463–478, https://doi.org/10.1038/s41578-019-0111-6.
[25] Y. Gu, J. Zhao, J.A. Johnson, Polymer networks: from plastics and gels to porous frameworks, Angew. Chem. Int. Ed. 59 (2020) 5022–5049, https://doi.org/10.1002/anie.201902900.
[26] K. Sano, Y. Ishida, T. Aida, Synthesis of anisotropic hydrogels and their applications, Angew. Chem. Int. Ed. 57 (2018) 2532–2543, https://doi.org/10.1002/anie.201708196.
[27] L. Zeng, X. Lin, P. Li, F.Q. Liu, H. Guo, W.-H. Li, Recent advances of organogels: from fabrications and functions to applications, Prog. Org. Coating 159 (2021), 106417, https://doi.org/10.1016/j.porgcoat.2021.106417.
[28] Z. Cao, H. Liu, L. Jiang, Transparent, mechanically robust, and ultrastable ionogels enabled by hydrogen bonding between elastomers and ionic liquids, Mater. Horiz. 7 (2020) 912–918, https://doi.org/10.1039/C9MH01699F.
[29] Y. Wang, L.-O. Heim, Y. Xu, G. Buntkowsky, K. Zhang, Transparent, stimuli-responsive films from cellulose-based organogel nanoparticles, Adv. Funct. Mater. 25 (2015) 1434–1441, https://doi.org/10.1002/adfm.201403067.
[30] G. Eke, N. Mangir, N. Hasirci, S. MacNeil, V. Hasirci, Development of a UV crosslinked biodegradable hydrogel containing adipose derived stem cells to promote vascularization for skin wounds and tissue engineering, Biomaterials 129 (2017) 188–198, https://doi.org/10.1016/j.biomaterials.2017.03.021.
[31] S. Panja, D.J. Adams, Stimuli responsive dynamic transformations in supramolecular gels, Chem. Soc. Rev. 50 (2021) 5165–5200, https://doi.org/10.1039/D0CS01166E.
[32] W. Lu, X. Le, J. Zhang, Y. Huang, T. Chen, Supramolecular shape memory hydrogels: a new bridge between stimuli-responsive polymers and supramolecular chemistry, Chem. Soc. Rev. 46 (2017) 1284–1294, https://doi.org/10.1039/C6CS00754F.
[33] S. Merino, C. Martín, K. Kostarelos, M. Prato, E. Vázquez, Nanocomposite hydrogels: 3D polymer–nanoparticle synergies for on-demand drug delivery, ACS Nano 9 (2015) 4686–4697, https://doi.org/10.1021/acsnano.5b01433.

[34] Y. Chen, S. Dai, H. Zhu, H. Hu, N. Yuan, J. Ding, Self-healing hydrogel sensors with multiple shape memory properties for human motion monitoring, New J. Chem. 45 (2021) 314–320, https://doi.org/10.1039/D0NJ04923A.
[35] Z. Zhao, K. Zhang, Y. Liu, J. Zhou, M. Liu, Highly stretchable, shape memory organohydrogels using phase-transition microinclusions, Adv. Mater. 29 (2017), 1701695, https://doi.org/10.1002/adma.201701695.
[36] S. Cai, B. Niu, X. Ma, S. Wan, X. He, High strength, recyclable, anti-swelling and shape-memory hydrogels based on crystal microphase crosslinking and their application as flexible sensor, Chem. Eng. J. 430 (2022), 132957, https://doi.org/10.1016/j.cej.2021.132957.
[37] C. Yan, Q. Yang, G. Li, A phenomenological constitutive model for semicrystalline two-way shape memory polymers, Int. J. Mech. Sci. 177 (2020), 105552, https://doi.org/10.1016/j.ijmecsci.2020.105552.
[38] X. Feng, G. Li, UV curable, flame retardant, and pressure-sensitive adhesives with two-way shape memory effect, Polymer 249 (2022), 124835, https://doi.org/10.1016/j.polymer.2022.124835.
[39] L. Ma, J. Zhao, X. Wang, M. Chen, Y. Liang, Z. Wang, Z. Yu, R.C. Hedden, Effects of carbon black nanoparticles on two-way reversible shape memory in crosslinked polyethylene, Polymer 56 (2015) 490–497, https://doi.org/10.1016/j.polymer.2014.11.036.
[40] S.J. Hong, W.R. Yu, J.H. Youk, Two-way shape memory behavior of shape memory polyurethanes with a bias load, Smart Mater. Struct. 19 (2010), 035022, https://doi.org/10.1088/0964-1726/19/3/035022.
[41] J.M. Raquez, S. Vanderstappen, F. Meyer, P. Verge, M. Alexandre, J.M. Thomassin, C. Jérôme, P. Dubois, Design of cross-linked semicrystalline poly(ε-caprolactone)-based networks with one-way and two-way shape-memory properties through diels-alder reactions, Chem. Eur J. 17 (2011) 10135–10143, https://doi.org/10.1002/chem.201100496.
[42] H. Qin, P.T. Mather, Combined one-way and two-way shape memory in a glass-forming nematic network, Macromolecules 42 (2009) 273–280, https://doi.org/10.1021/ma8022926.
[43] H.F. Lu, M. Wang, X.M. Chen, B.P. Lin, H. Yang, Interpenetrating liquid-crystal polyurethane/polyacrylate elastomer with ultrastrong mechanical property, J. Am. Chem. Soc. 141 (2019) 14364–14369, https://doi.org/10.1021/jacs.9b06757.
[44] C. Hao, K. Wang, Z. Wang, R. Duan, H. Liu, M. Huang, W. Liu, S. He, C. Zhu, Triple one-way and two-way shape memory poly(ethylene-co-vinyl acetate)/poly(ε-caprolactone) immiscible blends, J. Appl. Polym. Sci. 139 (2022), 51426, https://doi.org/10.1002/app.51426.